Author Manuscript

Author Manuscript

Author Manuscript

Author Manuscript

HHS Public Access

Author manuscript

Cell Rep. Author manuscript; available in PMC 2016 March 24.

Published in final edited form as:

Cell Rep. 2015 November 3; 13(5): 1046–1058. doi:10.1016/j.celrep.2015.09.063.

FOXC1 Activates Smoothened-Independent Hedgehog Signaling in Basal-like Breast Cancer

Bingchen Han[1], **Ying Qu**[1], **Yanli Jin**[1], **Yi Yu**[1], **Nan Deng**[2], **Kolja Wawrowsky**[3], **Xiao Zhang**[2], **Na Li**[4], **Shikha Bose**[5], **Qiang Wang**[6], **Sugunadevi Sakkiah**[3,6], **Ravinder Abrol**[3,6], **Tor W. Jensen**[7], **Benjamin Berman**[6], **Hisashi Tanaka**[1], **Jeffrey Johnson**[1], **Bowen Gao**[1], **Jijun Hao**[8], **Zhenqiu Liu**[2], **Ralph Buttyan**[4,9], **Partha S. Ray**[7], **Mien-Chie Hung**[10,11], **Armando E. Giuliano**[1], and **Xiaojiang Cui**[1,12]

[1]Department of Surgery, Samuel Oschin Cancer Institute, Cedars-Sinai Medical Center, Los Angeles, CA 90048, USA

[2]Biostatistics and Bioinformatics Research Center, Samuel Oschin Cancer Institute, Cedars-Sinai Medical Center, Los Angeles, CA 90048, USA

[3]Department of BioMedical Sciences, Samuel Oschin Cancer Institute, Cedars-Sinai Medical Center, Los Angeles, CA 90048, USA

[4]Vancouver Prostate Centre, University of British Columbia, Vancouver, BC V6H 3Z6, Canada

[5]Department of Pathology, Samuel Oschin Cancer Institute, Cedars-Sinai Medical Center, Los Angeles, CA 90048, USA

[6]Department of Medicine, Samuel Oschin Cancer Institute, Cedars-Sinai Medical Center, Los Angeles, CA 90048, USA

[7]Department of Surgery, University of Illinois College of Medicine at Urbana Champaign, Urbana, IL 61801, USA

[8]College of Veterinary Medicine, Western University of Health Sciences, Pomona, CA 91766, USA

Corresponding author: Xiaojiang Cui, 8700 Beverly Blvd, Davis Bldg 2065, Los Angeles, CA, USA. Phone: 310-423-7437; Fax: 310-423-9537; Xiaojiang.cui@cshs.org.

Publisher's Disclaimer: This is a PDF file of an unedited manuscript that has been accepted for publication. As a service to our customers we are providing this early version of the manuscript. The manuscript will undergo copyediting, typesetting, and review of the resulting proof before it is published in its final citable form. Please note that during the production process errors may be discovered which could affect the content, and all legal disclaimers that apply to the journal pertain.

Author Contributions

B.H. and X.C. conceived and designed the experiments. B.H. performed experiments unless specified. Y.Q., Y.J., Y.Y., B.G. and J.J. assisted with the experiments. X.Z., N.D., Z.L., B.B., and H.T. performed biostatistics and bioinformatics analysis. K.W. performed confocal and FRET experiments. Q.W., N.L., and R.B. assisted with protein interaction analysis. S.B. assisted with immunohistochemistry analysis. S.S. and R.A. performed protein structure analysis. J.H. assisted with Gli activity assays. T.W.J. and P.S.R. performed survival analysis. B.H. and X.C wrote, revised, and edited the manuscript. P.S.R, M.C.H., and A.E.G. participated in experimental design and manuscript preparation.

Accession Number

Microarray data reported in this paper is available in the NCBI GEO under accession number GEO: GSE73234.

Supplemental Information

Supplemental Information includes Supplemental Experimental Procedures, seven figures and three tables.

Author Manuscript Author Manuscript Author Manuscript Author Manuscript

[9]Department of Urologic Sciences, University of British Columbia, Vancouver, BC V6H 3Z6, Canada

[10]Department of Molecular and Cellular Oncology, the University of Texas MD Anderson Cancer Center, Houston, TX 77030, USA

[11]Center for Molecular Medicine and Graduate Institute of Cancer Biology, China Medical University, Taichung 402, Taiwan

[12]Department of Obstetrics and Gynecology, Samuel Oschin Cancer Institute, Cedars-Sinai Medical Center, Los Angeles, CA 90048, USA

Summary

The mesoderm- and epithelial-mesenchymal transition-associated transcription factor FOXC1 is specifically overexpressed in basal-like breast cancer (BLBC), but its biochemical function is not understood. Here we demonstrate that FOXC1 controls cancer stem cell (CSC) properties enriched in BLBC cells via activation of Smoothened (SMO)-independent Hedgehog (Hh) signaling. This non-canonical activation of Hh is specifically mediated by Gli2. We further show that the N-terminal domain of FOXC1 (aa 1–68) binds directly to an internal region (aa 898–1168) of Gli2, enhancing the DNA-binding and transcription-activating capacity of Gli2. FOXC1 expression correlates with that of Gli2 and its targets in human breast cancers. Moreover, FOXC1 overexpression reduces sensitivity to anti-Hedgehog (Hh) inhibitors in BLBC cells and xenograft tumors. Together, these findings reveal FOXC1-mediated non-canonical Hh signaling that determines the BLBC stem-like phenotype and anti-Hh sensitivity, supporting inhibition of FOXC1 pathways as potential approaches for improving BLBC treatment.

Keywords

basal-like breast cancer; cancer stem cells; FOXC1; Gli2; Hedgehog; Smoothened

Introduction

Breast cancer is a heterogeneous disease that consists of multiple molecular subtypes characterized by distinct pathophysiological features. By using high-throughput technologies, breast cancer has been classified into at least four biologically distinct subtypes: luminal A, luminal B, human epidermal growth factor receptor 2-overexpressing ($HER2^+$), and basal-like (Koboldt et al., 2012). Basal-like breast cancer (BLBC) accounts for 15–20% of all invasive breast cancers and is associated with high histologic grade, younger patient age, and poor prognosis (Rakha et al., 2008). Estrogen receptor-positive (ER^+) tumors of the luminal subtype can be treated with endocrine therapy, whereas $HER2^+$ tumors may benefit from antibody or small-molecule inhibitor drugs. In contrast, chemotherapy remains the only systemic treatment modality for BLBC.

Recent studies have shown that forkhead box C1 (FOXC1), a transcription factor involved in the development of mesoderm, brain, and eye during embryogenesis (Kume et al., 1998; Maclean et al., 2005), may serve as a key diagnostic biomarker specific for BLBC (Jensen et al., 2015; Ray et al., 2010). Elevated expression of FOXC1 also predicts poor overall

Author Manuscript Author Manuscript Author Manuscript Author Manuscript

survival in other cancers such as lung cancer (Wei et al., 2012) and hepatocellular carcinoma (Xia et al., 2013). A recent study has shown that NF-κB signaling mediates the function of FOXC1 in BLBC cell proliferation and invasion (Wang et al., 2012). Consistent with this result, matrix metalloprotease-7 (MMP7), which is regulated by NF-κB, mediates the invasion-promoting function of FOXC1 in BLBC (Sizemore and Keri, 2012).

Accumulating evidence indicates that cancer stem cells (CSCs) contribute to tumor growth, metastasis, and relapse, and that FOXC1 contributes to the CSC phenotype. Gene expression profiles suggest a less differentiated progenitor cell phenotype or a stem cell origin for BLBC (Ben-Porath et al., 2008; Zvelebil et al., 2013). In addition, BLBC is enriched with cells of the $CD44^+/CD24^-$ phenotype (Honeth et al., 2008), which possess tumor-initiating stem-like properties (Al-Hajj et al., 2003). A recent study showed that the FOXC1 protein is exclusively expressed in basal cells but that FOXC1 mRNA is enriched in luminal progenitor cells (Sizemore et al., 2013). In line with this finding, FOXC1 induces a progenitor-like phenotype in differentiated mammary epithelial cells (Bloushtain-Qimron et al., 2008). In tumor cells, FOXC1 can induce epithelial-mesenchymal transition (EMT) (Xia et al., 2013; Yu et al., 2013), a cellular feature associated with CSCs (Mani et al., 2008). Most recently, FOXC1 is reported to be a key regulator for development and maintenance of the mesenchymal niches for hematopoietic stem and progenitor cells (Omatsu et al., 2014). To date, it is unclear how FOXC1 interacts with or orchestrates signaling pathways involved in BLBC cell function and stem-like properties. To address this question, we explored the effects of FOXC1 on CSC properties *in vivo* and *in vitro* and the potential underlying mechanisms. We have identified FOXC1 as a Smoothened (SMO)-independent activator of Hedgehog (Hh) signaling via direct interaction with the Gli2 transcription factor. We also characterized the involvement of FOXC1 in the BLBC cell response to anti-SMO inhibitors.

Results

FOXC1 Increases CSC Properties in BLBC Cells *in vivo* and *in vitro*

Because FOXC1 emerges as a critical biomarker for BLBC and induces the CSC-associated EMT phenotype, we set out to directly test the effect of FOXC1 on CSC properties *in vivo* by performing limiting dilution injection experiments. FOXC1 was stably overexpressed in MDA-MB-231 cells (Figure S1A). Serial dilutions of control or FOXC1-overexpressing cells were injected orthotopically into the fourth mammary glands of BALB/c nude mice and tumor growth was examined. As presented in Figure 1A, there were no differences in the tumor incidence when 100,000 or 10,000 cells were injected. However, when as few as 1000 or 100 cells were inoculated, 7 or 3 out of 8 injections of FOXC1-overexpressing cells developed tumors respectively, as opposed to 2 or 0 out of 8 injections of control cells. Notably, when FOXC1-knockdown BT549 cells were injected into the mouse mammary glands, tumorigenesis was completely inhibited (Figure 1B).

CSC can also be identified by specific biomarkers *in vitro* in many types of cancer. Widely used biomarkers for characterizing breast CSC include elevated aldehyde dehydrogenase (ALDH) activity (Ginestier et al., 2007), $CD133^+$ (Wright et al., 2008), and $CD44^+/CD24^-$ (Al-Hajj et al., 2003). Breast CSC can also be propagated *in vitro* as mammospheres, which are spherical clusters of cells in non-adherent culture conditions (Ponti et al., 2005). Using

Author Manuscript Author Manuscript Author Manuscript Author Manuscript

the ALDEFLUOR assay followed by flow cytometry, we observed that ALDH activity was enhanced greater than 3-fold in FOXC1-overexpressing cells (Figure 1C). Conversely, when we knocked down FOXC1 using shRNAs in BT549 cells (Figure S1A), which express high levels of endogenous FOXC1, ALDH activity was dramatically reduced (Figure 1D). To further validate the effect of FOXC1 on ALDH activity in BLBC cells, we also overexpressed FOXC1 in SUM159 and MDA-MB-468 cells (Figure S1A). As expected, ALDH activity was significantly increased by FOXC1 in these two cell lines (Figure S1B). In agreement, knockdown of endogenous FOXC1 in SUM149 cells markedly inhibited ALDH activity (Figure S1A and B). The mammosphere formation ability of MDA-MB-231 cells was substantially increased by FOXC1 overexpression (Figure 1E). Similar results were found in FOXC1-overexpressing SUM159 cells (Figure S1C). Of note, mammosphere growth was abolished by FOXC1-knockdown in BT549 cells (Figure 1F). Likewise, mammosphere formation in FOXC1-knockdown SUM149 cells was also repressed (Figure S1C).

We also examined the effect of FOXC1 expression on the $CD133^+$ population. As shown in Figure S1D, overexpression of FOXC1 increased the $CD133^+$ population in both MDA-MB-231 and SUM159 cells, whereas knockdown of FOXC1 reduced the $CD133^+$ population in both BT549 and SUM149 cells. We further explored the regulation of the $CD44^+CD24^-$ breast CSC marker. Although no changes were observed in FOXC1-overexpressing MDA-MB-468 or FOXC1-knockdown BT549 cells, the $CD44^+CD24^-$ population was indeed increased by FOXC1 overexpression in SUM159 cells (Figure S1E). Conversely, knockdown of FOXC1 reduced the population in SUM149 cells (Figure S1E). Of note, parental BT549 and MDA-MB-231 cells showed high $CD44^+CD24^-$ populations (Figure S1E), as described previously (Ricardo et al., 2011), suggesting that these subpopulations may not represent CSCs in the two cell lines. Taken together, these results demonstrate that FOXC1 positively regulates CSC properties of BLBC cells *in vivo* and *in vitro*.

It has been reported that transformation from a luminal primary to a basal-like recurrence is more likely than the opposite phenomena (Castaneda et al., 2012). Recent studies showed that FOXC1 is associated with mesenchymal circulating tumor cells from both ER^+ and ER^- breast cancer and may induce EMT in ER^+ breast cancer cells (Yu et al., 2013). Thus, we explored the effect of FOXC1 on CSC properties in two ER^+ cell lines, MCF7 and T47D, which harbor undetectable FOXC1 levels (Figure S1A). Likewise, FOXC1 overexpression in these cells increased ALDH activity (Figure S1B), mammosphere formation (Figure S1C) and the $CD44^+CD24^-$ population (Figure S1E), but not the $CD133^+$ cell percentage (Figure S1D). Together, these results further substantiate a role of FOXC1 in CSCs.

FOXC1 Activates SMO-independent Hedgehog Signaling in BLBC Cells

Studies have shown that CSCs share many features with normal stem cells, including self-renewal and differentiation as well as the signaling mechanisms governing the stemness property (Magee et al., 2012). Three well-known classical signaling pathways involved in the normal stem cell function are the Wnt, Hh, and Notch pathways, which are also implicated in breast cancer development and CSC maintenance (Lobo et al., 2007). Hence,

Author Manuscript Author Manuscript Author Manuscript Author Manuscript

we first examined whether FOXC1 can activate these pathways. To do this, we performed pathway-specific binding site luciferase reporter assays, which measure the extent of activation of these three pathways. As shown in Figure 2A, FOXC1 potently induced Hh-responsive luciferase (8×3′Gli-binding site (BS)-luciferase) (Sasaki et al., 1997) activity in different BLBC cell lines. Similar results were observed in MCF7 and T47D cells (Figure S2A). In contrast, FOXC1 did not significantly induce Wnt or Notch pathway-specific luciferase activity (Figure S2B and C).

To confirm the activation of Hh signaling by FOXC1, we examined the expression of genes known to be induced by the activation of the Hh signaling. Using real-time PCR assays, we found that the mRNA levels of *human hedgehog interacting protein* (*Hhip*) and *Patched1* (*Ptch1*) were significantly up-regulated by FOXC1 in different BLBC cell lines (Figure 2B). In support of these observations, higher levels of endogenous FOXC1 were found to be associated with more robust Gli-BS luciferase activity in multiple breast cancer cell lines, which were transfected with the same amount of the 8×3′Gli-BS-luciferase construct (Figure 2C). Taken together, these results demonstrate that FOXC1 activates the Hh signaling pathway in BLBC cells.

In canonical mammalian Hh signaling, SMO is the central signal transducer (Robbins et al., 2012). Surprisingly, SMO mRNA and protein were not detected in MDA-MB-231 or HCC1500 cells, even though FOXC1 activates Hh signaling in these two cell lines (Figure 2D). On the other hand, although SUM159 and SUM1315 cells express readily detectable SMO (Figure 2D), FOXC1-induced Gli-BS-luciferase activity was not affected by siRNA-mediated SMO knockdown (Figure 2E and F). Similar results were found in luminal MCF7 and T47D cells (Figure S2D and E). To substantiate these results, we examined the effects of the two SMO inhibitors GDC-0449 (Vismodegib) and LDE225 (Sonidegib) on FOXC1-induced Hh signaling. As expected, neither of them reduced FOXC1-induced Gli-BS-luciferase activity in SMO-positive (SUM159 and T47D) or SMO-negative (MDA-MB-231 and MCF7) breast cancer cells (Figure 2G and H, S2F and G). On the contrary, when the cells were treated with another Hh pathway inhibitor, GANT61, which directly targets the DNA-binding ability of Gli proteins (Lauth et al., 2007), FOXC1-induced Gli-BS-luciferase activity was considerably attenuated (Figure 2I and S2H). To further verify that FOXC1 activates SMO-independent Hh signaling, we treated SHH-Light2, a clonal NIH3T3 cell line stably transfected with 8×3′Gli-BS-luciferase construct (Taipale et al., 2000), with Hh signaling agonist amino-terminal domain of SHH (SHH-N). FOXC1 significantly induced luciferase activity when SMO was inhibited by GDC-0449 (Figure 2J) or LDE225 (Figure 2K). These results demonstrate that FOXC1-induced activation of Hh signaling in BLBC cells is SMO-independent.

Gli2 Mediates FOXC1-induced CSC Properties

The ultimate effectors in the mammalian Hh signaling are the three transcription factors Gli1, Gli2, and Gli3. They bind directly to gene promoters through zinc-finger motifs and regulate the expression of target genes involved in diverse cell functions (Hui and Angers, 2011). To determine their individual role in the FOXC1-induced activation of Hh signaling, we knocked down the expression of Gli1, Gli2, or Gli3 in MDA-MB-231 cells using

Author Manuscript Author Manuscript Author Manuscript Author Manuscript

siRNAs (Figure S3A). Interestingly, only Gli2, but not Gli1 or Gli3 knockdown, decreased FOXC1-induced Gli-BS-luciferase activity (Figure 3A, Figure S3B and C) as well as *Hhip* and *Ptch1* mRNA expression levels (Figure 3B). To corroborate that Gli2 is responsible for the activation of Hh signaling by FOXC1, we treated cells with arsenic trioxide (ATO), which inhibits Hh signaling by preventing Gli2 ciliary accumulation and promoting its degradation (Kim et al., 2010). As illustrated in Figure S3D and E, ATO inhibited FOXC1-induced Gli-BS-luciferase activity and *Hhip* and *Ptch1* mRNA expression. These results implicate Gli2 as a mediator of FOXC1-induced activation of Hh signaling.

We proceeded to determine whether the induction of CSC properties by FOXC1 in BLBC cells is mediated by Gli2. For this purpose, we repressed Gli2 expression using shRNAs in FOXC1-overexpressing MDA-MB-231 cells (Figure S3F). The ALDEFLUOR assay showed that elevated ALDH activity and mammosphere formation capacity in FOXC1-overexpressing cells were markedly suppressed by Gli2 knockdown (Figure 3C and E). Likewise, when Gli2 was knocked down in BT549 cells (Figure S3G), ALDH activity and mammosphere growth were markedly reduced (Figure 3D and F), which resembles the effects of FOXC1-knockdown on ALDH activity and mammosphere growth in BT549 cells (Figure 1D and F). We next re-expressed mouse Gli2, whose expression was not affected by human Gli2 shRNA, in the Gli2-knockdown FOXC1-overexpressing MDA-MB-231 cells. As shown in Figure S3H and I, the Gli2-knockdown-induced decrease of ALDH activity and mammosphere growth was partially rescued by mouse Gli2 overexpression. Next, we injected different numbers of control or Gli2-knockdown FOXC1-overexpressing MDA-MB-231 cells into the mammary fat pads of BALB/c nude mice. The results showed that Gli2 knockdown attenuated FOXC1-induced tumorigenicity (Figure 3G). Taken together, these results suggest that Gli2 is a critical mediator of the effects of FOXC1 on tumorigenesis and CSC properties of breast cancer cells.

FOXC1 Interacts with Gli2 in BLBC Cells

Next we investigated how FOXC1 engages Gli2 in its regulation of breast CSC properties. Because activation of SMO-independent Hh signaling can be induced by up-regulation of Gli expression (Lauth and Toftgard, 2007), we first tested whether FOXC1 regulates Gli2 expression in breast cancer cells. Real-time PCR and western blotting analysis showed that FOXC1 did not affect Gli2 mRNA or protein levels in MDA-MB-231 cells (Figure S4A and B). Furthermore, western blotting of cytoplasmic and nuclear lysates and immunofluorescence staining indicated that FOXC1 did not alter the intracellular distribution of the Gli2 protein, which was mainly localized in the nucleus in both control and FOXC1-overexpressing MDA-MB-231 cells (Figure S4C and D).

Given that both FOXC1 and Gli2 are transcription factors, we assessed whether these two proteins can interact with each other. To address this question, we transfected both FOXC1 and Gli2 constructs into HEK293T cells, and performed immunoprecipitation (IP) assays. As shown in Figure 4A, overexpressed FOXC1 and Gli2 were co-immunoprecipitated from HEK293T cells with anti-FOXC1 or anti-Gli2 antibodies. Similar results were found in FOXC1-overexpressing MDA-MB-231 cells with relatively high levels of endogenous Gli2 (Figure 4B). In addition, co-IP of the two proteins was also detected in BT549 cells, which

Author Manuscript Author Manuscript Author Manuscript Author Manuscript

possess high levels of both endogenous FOXC1 and Gli2 (Figure 4C). Consistent with our results, co-IP of FOXC1 and Gli2 has been recently reported in a study of endochondral ossification (Yoshida et al., 2015).

To test whether the binding between these two proteins is direct, which no other factors are involved, we expressed His-tagged-FOXC1 and glutathione S-transferase (GST) tagged-Gli2 in E. coli BL21 (DE3) and performed GST and His pull-down assays. As presented in Figure 4D (left), the GST-Gli2 bait interacted directly with His-FOXC1. Reciprocally, the His-FOXC1 bait captured GST-Gli2 (Figure 4D, right). To confirm the direct interaction of these two proteins, we performed the fluorescence resonance energy transfer (FRET) assay, which is commonly used to assess the proximity of two proteins. As demonstrated in Figure 4E, a significant increase in donor fluorescence was found after bleaching acceptor fluorescence, suggesting that FRET occurred between FOXC1 and Gli2. We measured FRET efficiency for each individual cell. The measured FRET efficiency was 50% ± 3% (n = 15) (Table S1), indicating consistently high proximity of the proteins in the cells. In agreement with the above results, colocalization was observed in the nucleus of HEK293T cells transfected with FOXC1 and Gli2 (Figure S4E). These data suggest that FOXC1 and Gli2 bind directly to each other in BLBC cells.

Next we aimed to identify the FOXC1 domain that participates in this interaction. With this in view, we constructed His-tagged expression vectors for truncated FOXC1 mutants comprising the N-terminal, DNA-binding, transcription-inhibitory and C-terminal domains (Berry et al., 2002) (Figure 4F left). These constructs and GST-Gli2 were expressed in E. coli BL21 (DE3) and proteins were purified, followed by co-immunoprecipitation (co-IP) assays. Western blotting results showed that only the FOXC1 mutants containing the N-terminal domain (aa 1–68), but not other mutants, bind directly to the Gli2 protein (Figure 4F right). We also constructed mammalian expression vectors for Myc-tagged truncated FOXC1 mutants and ectopically expressed them in MDA-MB-231 cells (Figure S4F). Likewise, the FOXC1 fragment of aa 1–178, which contains the N-terminal domain (aa 1–68), was found to interact with endogenous Gli2 (Figure S4G). Of note, the expression of the N-terminal domain (aa 1–168) was not detectable in MDA-MB-231 cells. Alternatively, this fragment was fused with GFP and successfully overexpressed in MDA-MB-231 cells (Figure S4H). As expected, the FOXC1 protein fragment was co-immunoprecipitated with Gli2 (Figure S4H). In line with these results, luciferase assays revealed that the FOXC1 mutants comprising aa 1–68 induced Gli-BS-luciferase activity similar to the full-length FOXC1 (Figure S4I). Taken together, these data demonstrate that FOXC1 directly interacts with Gli2 via its N-terminal domain (aa 1–68).

We then proceeded to identify the Gli2 domain involved in the binding to FOXC1. The Gli2 protein consists of an N-terminal domain, a zinc finger DNA-binding domain, and a C-terminal domain (Figure 4G, left) (Li et al., 2014). We constructed mammalian expression vectors for Myc-tagged truncated Gli2 mutants. These constructs were transfected into HEK293T cells together with FOXC1, followed by co-IP assays. Western blotting results indicated that only the Gli2 constructs containing aa 898–1168, but not other constructs, bound to FOXC1 (Figure 4G, right). Using site-directed mutagenesis, we also generated a mutant mouse Gli2 that lacks aa 891–1154, corresponding to human Gli2 aa 898–1168. As

Author Manuscript Author Manuscript Author Manuscript Author Manuscript

expected, this Gli2 deletion mutant could not rescue the Gli2 knockdown-elicited phenotypes of ALDH activity and mammosphere formation (Figure S3H and I). These results suggest that the aa 898–1168 region in Gli2 mediates its binding to FOXC1.

Gli1 and Gli2 are the two major mediators for Hh-induced gene transcription. We have shown that Gli1 is not involved in the effect of FOXC1 on transcriptional activity of Gli proteins (see Figure 3A), suggesting that FOXC1 may not interact with Gli1. To corroborate this, we transfected HEK293T cell with both FOXC1 and Gli1 and then performed co-IP assay. As shown in Figure S4J, no interaction was detected between the two proteins. We also compared the sequence of Gli2 (aa 898–1168) with the corresponding region of Gli1 and found no significant homology between the two regions (Figure S4K).

Structural Model of FOXC1-Gli2 Interaction

We then used the above interaction information to construct an atomistic model of the interaction interface in the proposed FOXC1-Gli2 complex (see Supplemental Experimental Procedures for details). The top four interaction poses by energy of $FOXC1^{1–68}4$ with $Gli2^{898–1168}$ are shown in Figure S5A (referred to as *4_10, 4_64, 4_68, 4_77*). Table S2 lists all the favorable interactions seen in these four interaction models. Models *4_64, 4_68,* and *4_77* are similar to each other and different from model 4_10. Model 4_77 was chosen for mutagenesis experiments because, of the four best models chosen by energy, it had the most interactions (Table S2). The residues chosen for mutation are shown in Figure S5B by gray boxes. To validate the computational structural model of the interaction, we constructed the mutant shown in Figure S5B based on model *4_77* and performed co-IP assays. As predicted, no interaction was observed between FOXC1 and mutant Gli2 (aa 898–1168) when FOXC1 and Myc tag antibodies were used to immunoprecipitate the FOXC1 protein and the Gli2 fragment, respectively (Figure S5E), indicating the critical role of the mutated residues in the FOXC1-Gli2 interaction. These residues provide structural hints and complex 4_77 provides an informative structural model for the direct interaction observed in this study between FOXC1 and Gli2.

Furthermore, structural modeling showed that the binding of FOXC1 to Gli2 can allosterically change (open) the DNA binding domain of Gli2 (Figure S5F), providing a structural hypothesis for how FOXC1 binding to Gli2 can potentially promote the DNA binding capacity of Gli2.

FOXC1 Promotes the DNA-binding Ability of Gli2 in BLBC Cells

Next, we examined whether FOXC1 enhances the DNA-binding ability of Gli2. It was noted that there is a consensus Gli2-binding site GACCACCCA in the promoter of *FAM38B* gene, which was markedly up-regulated by FOXC1 overexpression in MDA-MB-231 cells as revealed by microarray assays (GEO: GSE73234). Using the chromatin immunoprecipitation (ChIP) assay, we found that FOXC1 enhanced the binding of Gli2 to the *FAM38B* promoter in MDA-MB-231 cells, and this enhancement was eliminated by Gli2-knockdown (Figure 5A). Next, we performed the electrophoretic mobility shift assay (EMSA) assay. Synthesized biotin-labeled 21bp oligos containing the wild-type or mutant Gli2-binding site in the *FAM38B* promoter were used as the probes. As shown in Figure 5B,

Author Manuscript Author Manuscript Author Manuscript Author Manuscript

FOXC1 overexpression led to an upward mobility shift of oligos in gels, reflecting increased binding of Gli2 to the biotin-labeled oligos. FOXC1-induced augmentation of Gli2 DNA-binding capacity was further substantiated by the biotinylated oligonucleotide precipitation assay. Using the biotin-labeled oligonucleotides comprising the Gli2 binding site from the *FAM38B* promoter, Gli2 was found to be pulled down with FOXC1 in FOXC1-overexpressing MDA-MB-231 cells (Figure 5C, left). Similar result was found when MDA-MB-231 cells were transfected with the FOXC1 fragment (aa 1–178), which comprises the Gli2-binding (aa 1–68) and DNA-binding (forkhead) domains (Figure 5C, right). However, overexpression of the FOXC1 fragment of aa 367–553, which is not involved in the binding of FOXC1 to Gli2, did not induce the binding of Gli2 to the biotin-oligos (Figure 5C, right). These data indicate that FOXC1 promotes the DNA-binding capacity of Gli2 in breast cancer cells.

Expression of FOXC1 Correlates with the Activation of the Hedgehog Signaling in Clinical Samples

To assess the clinical significance of FOXC1-induced activation of the Hh signaling, we evaluated the expression levels of FOXC1 and Gli2 using immunohistochemistry (IHC) in human breast cancers. Because FOXC1 is specifically expressed in BLBC or triple-negative breast cancer (TNBC) and the majority of TNBC display a basal-like phenotype (Han et al., 2013), we performed IHC staining on TNBC tissue microarrays. FOXC1 and Gli2 were readily detectable in 54.2% and 81.3% of cases, respectively, and a strong correlation between the expressions of the two proteins was found (Figure 6A and B). We also evaluated the expression of Ptch1 and Hhip proteins. Significant correlations were also observed between FOXC1 and Ptch1 as well as between FOXC1 and Hhip (Figure 6A, C and D). Analysis of The Cancer Genome Atlas (TCGA) database and Curtis dataset (Curtis et al., 2012) showed that the mRNA levels of FOXC1 strongly correlate with those of Gli2 and Ptch1 in breast cancer samples (Figure 6E and S6A). Even though the correlation between FOXC1 and Hhip was not statistically significant in TCGA samples, a significant association between them was observed in a Singapore cohort dataset (Figure S6C). We also performed multiple regression analysis which incorporated 13 Hh pathway-associated genes (See Statistics in Supplemental Experimental Procedures) in the three cohort datasets. A strong correlation between FOXC1 levels and Hh pathway activation was found in all three datasets (Figure 6F, S6B and D). We further tested whether the Hh gene signature correlates with breast cancer prognosis. Using K-means clustering, two groups of patients with either positively (n=378) or negatively (n=1608) enriched Hh pathway-associated genes were found in the Curtis dataset. As illustrated in Figure 6G, the former group was associated with elevated FOXC1 expression levels (47.03 ± 2.98 vs 8.54 ± 0.36, $p < 0.0001$) and decreased disease-specific survival that was statistically significant compared to the latter group (HR = 1.973, 95% CI = 1.802 to 2.961, $p < 0.0001$). Taken together, these data suggest a positive correlation between FOXC1 and the activation of Hh signaling in clinical samples.

FOXC1 Reduces Sensitivity to Anti-SMO Drugs in BLBC Cells

Since the Hh signaling is critically involved in tumorigenesis and CSC function, many efforts have gone into developing anti-Hh inhibitors for anti-cancer therapy. GDC-0449, a

Author Manuscript Author Manuscript Author Manuscript Author Manuscript

SMO-targeting inhibitor, has been approved by FDA for the treatment of basal cell carcinoma. Hh inhibition is also in clinical trials for triple-negative breast cancers (ClinicalTrials.gov, NCT01757327). Because FOXC1 activates Hh signaling via a SMO-independent manner, we reasoned that elevated expression of FOXC1 may render cancer cells refractory to SMO-targeting inhibitors. To address this question, we analyzed the effects of GDC-0449 on cell viability in control and FOXC1-overexpressing BLBC cells. Cell viability assays showed that elevated expression of FOXC1 reduced the sensitivity to GDC-0449 in different SMO-positive BLBC cell lines (Figure 7A–D). In agreement with this result, the mRNA expression levels of *Ptch1* and *Hhip* were inhibited by GDC-0449 in these cells, and this GDC-0449 effect was attenuated by FOXC1 overexpression (Figure S7A). We also generated GDC-0449-resistant BLBC sublines by long-term culture of parental cells in the presence of increasing concentrations of GDC-0449. As illustrated in Figure 7E, the derived GDC-0449-resistant cells possessed higher expression levels of FOXC1. Interestingly, when FOXC1 was repressed by siRNAs in these cells, the acquired GDC-0449 resistance was attenuated (Figure S7B–E). We then tested the effect of FOXC1 on GDC-0449-induced tumor growth inhibition *in vivo* by orthotopic injection of control and FOXC1-overexpressing MDA-MB-468 cells into the mouse mammary glands. As shown in Figure 7F, GDC-0449 impeded the growth of control group tumors, whereas overexpression of FOXC1 abolished this inhibitory effect. Taken together, these results indicate that the expression of FOXC1 renders cancer cells refractory to SMO-targeting drugs, which has clinical implications for ongoing investigations of anti-Hh inhibitors in breast cancer therapy.

Discussion

BLBC has been shown to possess intrinsic CSC properties (Ben-Porath et al., 2008; Honeth et al., 2008), which may explain in part the aggresive clinical behavior of this breast cancer subtype. The findings reported in this study provide a mechanism underlying the aggressiveness and poor prognosis of BLBC and establish FOXC1 as a promising therapeutic target for BLBC treatment. Interestingly, FOXC2, another member of the FOX family, has also been shown to regulate CSCs in breast cancer (Hollier et al., 2013), emphasizing the involvement of FOXC members in the regulation of breast CSCs.

One novel aspect of our study is the finding that FOXC1 activates SMO-independent Hh signaling through direct interaction with Gli2, mediating the effect of FOXC1 on CSC properties in BLBC cells. A more in-depth mechanism of how FOXC1 binding elicits enhanced Gli2 DNA-binding ability remains to be determined. Previous studies have reported that Hh signaling is associated with BLBC (O'Toole et al., 2011) and breast cancer progression (Kubo et al., 2004). It is also essential for maintenance of CSCs (Coni et al., 2013) and is hyperactive in breast CSCs with the $CD44^+/CD24^-$ phenotype (Liu et al., 2006). On the basis of these studies, we propose a model of the FOXC1-Gli2 signaling axis as a key regulator for breast CSCs (Figure 7G).

The canonical Hh pathway is activated upon Hh ligand binding to the cognate receptor Ptch1, which enables SMO to activate Gli proteins. Hh signaling can also be activated in a non-canonical manner. For example, transforming growth factor β (TGFβ) can activate the

Author Manuscript Author Manuscript Author Manuscript Author Manuscript

Hh pathway by inducing Gli2 expression (Dennler et al., 2007). Similarly, mutant KRAS can induce Gli1 and Gli2 expression independent of SMO in pancreatic cells (Ji et al., 2007). Moreover, in esophageal adenocarcinoma, mTOR/S6K1 pathway activates Hh signaling through eliciting SMO-independent Gli1 translocation into the nucleus (Wang et al., 2012a). Distinct from the above reports, our study provides a new non-canonical Hh signaling activation mechanism mediated by transcription factor interaction.

Much effort has been directed toward the development of anti-Hh drugs for cancer therapy. One of the most widely used drugs for targeting the Hh pathway is GDC-0449, the first drug approved by the FDA to treat basal cell carcinoma (BCC). Several other small-molecule inhibitors such as LDE225 and IPI-926 (Saridegib) are also being evaluated in clinical trials (Low and de Sauvage, 2010). It merits mentioning that all of these drugs target SMO and, to date, appear to be largely ineffective in solid tumors other than BCC (Kaye et al., 2012). Our study demonstrates that FOXC1 activates Hh signaling independently of SMO and thereby induces resistance to SMO inhibitors in BLBC cells. As such, agents that target the Hh pathway downstream of SMO by directly blocking Gli function may be effective to reverse the SMO inhibitor resistance driven by SMO-independent Gli activation. Indeed, Gli-inhibiting compounds itraconazole and arsenic trioxide retain Hh-inhibitory activity in anti-SMO-resistant tumors (Kim et al., 2013), consistent with our finding that GANT61 and ATO inhibit FOXC1-elicited Hh signaling activation. Moreover, our findings that FOXC1 is up-regulated in SMO inhibitor-resistant BLBC cell models and involved in clinical drug resistance further implicate FOXC1 in SMO inhibitor treatment failure.

It is noted that LDE225 is already undergoing clinical trials for ER^- and $HER2^-$ breast cancers (ClinicalTrials.gov, NCT01757327). However, current findings allow for reasonable speculation that LDE225 and other similar drugs may not be effective against cancers expressing high levels of FOXC1. Because FOXC1 is also overexpressed in other cancers, it may serve as a marker for selecting patients who do not benefit from anti-SMO therapies, and as a target for overcoming anti-Hh drug resistance.

In summary, we have uncovered a FOXC1-mediated, SMO-independent Hh signaling mechanism that regulates CSC properties and anti-Hh/SMO drug resistance. This data further supports a critical role of FOXC1 in BLBC and warrants continued investigation of FOXC1 as a new avenue for BLBC treatment.

Experimental Procedures

Cell culture

Human breast cancer cell lines and HEK293T cells were acquired from American Type Culture Collection (ATCC) and maintained according to ATCC instructions.

Flow cytometry (FACS)

Approximately 2×10^5 cells were suspended in FACS buffer (1×PBS, 1% BSA) and incubated with antibodies at 4°C for 30min. Detection of ALDH activity was performed using the ALDEFLUOR Assay Kit (StemCell Technologies) according to the

Author Manuscript Author Manuscript Author Manuscript Author Manuscript

manufacturer's instruction. Please see "Supplemental Experimental Procedures" for detailed information.

Chromatin immunoprecipitation (ChIP)

Approximately 5×10^6 cells were collected and ChIP assays were performed using the EZ-ChIP Chromatin Immunoprecipitation Kit (EMD Millipore) according to the manufacturer's instructions. Gli2 antibody (sc-28674, Santa Cruz) -immunoprecipitated DNA was analyzed by RT- PCR and real-time PCR. The primers were: *FAM38B*-forward: 5′-TACATACGTTGGAAGTCTCAG-3′, *FAM38B*-reverse: 5′-CAAGATTCCCAGCAGGTG-3′.

Immunofluorescence (IF) and fluorescence resonance energy transfer (FRET)

Cells were placed into chamber slides (Thermo) at 70–80% confluence. Cells were fixed, permeabilized and incubated with primary and secondary antibodies. Images were acquired with Leica SP5 X confocal microscope (Leica Microsystems). Please see "Supplemental Experimental Procedures" for detailed information.

Biotinylated oligonucleotide precipitation assay

The 5′-biotinylated oligonucleotides were synthesized from Invitrogen. Complementary oligonucleotides were annealed. Nuclear proteins were extracted using NE-PER Nuclear and Cytoplasmic Extraction Reagents (Thermo). Biotinylated double-stranded oligonucleotides were incubated with nuclear proteins. DNA-bound proteins were precipitated using Streptavidin Agarose Beads (Thermo). Please see "Supplemental Experimental Procedures" for detailed information.

Supplementary Material

Refer to Web version on PubMed Central for supplementary material.

Acknowledgments

We thank Sandra Orsulic for providing the pEGFP-C3 plasmid, Wolf Wiedemeyer for providing the pBABE-puro plasmid, Hiroshi Sasaki for providing wild-type and mutant 8×3′Gli-BS-luciferase constructs (Kumamoto University). This work was supported by National Institutes of Health (CA151610), the Avon Foundation (02-2014-063), David Salomon Translational Breast Cancer Research Fund, the Fashion Footwear Charitable Foundation of New York, Inc. and the Margie and Robert E. Petersen Foundation. X. Cui and P. Ray are named inventors on patent applications regarding the role of FOXC1 in cancer. P. Ray has stock ownership in Onconostic Technologies, Inc. The other authors declare that no conflict of interest exists.

References

Al-Hajj M, Wicha MS, Benito-Hernandez A, Morrison SJ, Clarke MF. Prospective identification of tumorigenic breast cancer cells. Proc Natl Acad Sci USA. 2003; 100:3983–3988. [PubMed: 12629218]

Ben-Porath I, Thomson MW, Carey VJ, Ge R, Bell GW, Regev A, Weinberg RA. An embryonic stem cell-like gene expression signature in poorly differentiated aggressive human tumors. Nat Genet. 2008; 40:499–507. [PubMed: 18443585]

Berry FB, Saleem RA, Walter MA. FOXC1 transcriptional regulation is mediated by N- and C-terminal activation domains and contains a phosphorylated transcriptional inhibitory domain. J Biol Chem. 2002; 277:10292–10297. [PubMed: 11782474]

Author Manuscript Author Manuscript Author Manuscript Author Manuscript

Bloushtain-Qimron N, Yao J, Snyder EL, Shipitsin M, Campbell LL, Mani SA, Hu M, Chen H, Ustyansky V, Antosiewicz JE, et al. Cell type-specific DNA methylation patterns in the human breast. Proc Natl Acad Sci USA. 2008; 105:14076–14081. [PubMed: 18780791]

Castaneda CA, Andres E, Barcena C, Gomez HL, Cortes-Funes H, Ciruelos E. Behaviour of breast cancer molecular subtypes through tumour progression. Clin Transl Oncol. 2012; 14:481–485. [PubMed: 22634538]

Coni S, Infante P, Gulino A. Control of stem cells and cancer stem cells by Hedgehog signaling: pharmacologic clues from pathway dissection. Biochem Pharmacol. 2013; 85:623–628. [PubMed: 23148911]

Curtis C, Shah SP, Chin SF, Turashvili G, Rueda OM, Dunning MJ, Speed D, Lynch AG, Samarajiwa S, Yuan Y, et al. The genomic and transcriptomic architecture of 2,000 breast tumours reveals novel subgroups. Nature. 2012; 486:346–352. [PubMed: 22522925]

Dennler S, Andre J, Alexaki I, Li A, Magnaldo T, ten Dijke P, Wang XJ, Verrecchia F, Mauviel A. Induction of sonic hedgehog mediators by transforming growth factor-beta: Smad3-dependent activation of Gli2 and Gli1 expression *in vitro* and *in vivo*. Cancer Res. 2007; 67:6981–6986. [PubMed: 17638910]

Ginestier C, Hur MH, Charafe-Jauffret E, Monville F, Dutcher J, Brown M, Jacquemier J, Viens P, Kleer CG, Liu S, et al. ALDH1 is a marker of normal and malignant human mammary stem cells and a predictor of poor clinical outcome. Cell Stem Cell. 2007; 1:555–567. [PubMed: 18371393]

Han, BC.; Audeh, W.; Jin, YL.; Bagaria, SP.; Cui, XJ. Biology and treatment of basal-like breast cancer Cell and Molecular Biology of Breast Cancer. Schatten, H., editor. New York, USA: Springer Humana Press; 2013. p. 91-109.

Hollier BG, Tinnirello AA, Werden SJ, Evans KW, Taube JH, Sarkar TR, Sphyris N, Shariati M, Kumar SV, Battula VL, et al. FOXC2 expression links epithelial-mesenchymal transition and stem cell properties in breast cancer. Cancer Res. 2013; 73:1981–1992. [PubMed: 23378344]

Honeth G, Bendahl PO, Ringner M, Saal LH, Gruvberger-Saal SK, Lovgren K, Grabau D, Ferno M, Borg A, Hegardt C. The CD44+/CD24− phenotype is enriched in basal-like breast tumors. Breast Cancer Res. 2008; 10:R53. [PubMed: 18559090]

Hui CC, Angers S. Gli proteins in development and disease. Annu Rev Cell Dev Biol. 2011; 27:513–537. [PubMed: 21801010]

Jensen TW, Ray T, Wang J, Li X, Naritoku WY, Han B, Bellafiore F, Bagaria SP, Qu A, Cui X, et al. Diagnosis of Basal-Like Breast Cancer Using a FOXC1-Based Assay. J Natl Cancer Inst. 2015; 107:djv148. [PubMed: 26041837]

Ji Z, Mei FC, Xie J, Cheng X. Oncogenic KRAS activates hedgehog signaling pathway in pancreatic cancer cells. J Biol Chem. 2007; 282:14048–14055. [PubMed: 17353198]

Kaye SB, Fehrenbacher L, Holloway R, Amit A, Karlan B, Slomovitz B, Sabbatini P, Fu L, Yauch RL, Chang I, et al. A phase II, randomized, placebo-controlled study of vismodegib as maintenance therapy in patients with ovarian cancer in second or third complete remission. Clin Cancer Res. 2012; 18:6509–6518. [PubMed: 23032746]

Kim J, Aftab BT, Tang JY, Kim D, Lee AH, Rezaee M, Chen B, King EM, Borodovsky A, Riggins GJ, et al. Itraconazole and arsenic trioxide inhibit Hedgehog pathway activation and tumor growth associated with acquired resistance to smoothened antagonists. Cancer Cell. 2013; 23:23–34. [PubMed: 23291299]

Kim J, Lee JJ, Gardner D, Beachy PA. Arsenic antagonizes the Hedgehog pathway by preventing ciliary accumulation and reducing stability of the Gli2 transcriptional effector. Proc Natl Acad Sci USA. 2010; 107:13432–13437. [PubMed: 20624968]

Koboldt DC, Fulton RS, McLellan MD, Schmidt H, Kalicki-Veizer J, McMichael JF, Fulton LL, Dooling DJ, Ding L, Mardis ER, et al. Comprehensive molecular portraits of human breast tumours. Nature. 2012; 490:61–70. [PubMed: 23000897]

Kubo M, Nakamura M, Tasaki A, Yamanaka N, Nakashima H, Nomura M, Kuroki S, Katano M. Hedgehog signaling pathway is a new therapeutic target for patients with breast cancer. Cancer Res. 2004; 64:6071–6074. [PubMed: 15342389]

Author Manuscript Author Manuscript Author Manuscript Author Manuscript

Kume T, Deng KY, Winfrey V, Gould DB, Walter MA, Hogan BL. The forkhead/winged helix gene Mf1 is disrupted in the pleiotropic mouse mutation congenital hydrocephalus. Cell. 1998; 93:985–996. [PubMed: 9635428]

Lauth M, Bergstrom A, Shimokawa T, Toftgard R. Inhibition of GLI-mediated transcription and tumor cell growth by small-molecule antagonists. Proc Natl Acad Sci USA. 2007; 104:8455–8460. [PubMed: 17494766]

Lauth M, Toftgard R. Non-canonical activation of GLI transcription factors: implications for targeted anti-cancer therapy. Cell Cycle. 2007; 6:2458–2463. [PubMed: 17726373]

Li N, Chen M, Truong S, Yan C, Buttyan R. Determinants of Gli2 co-activation of wildtype and naturally truncated androgen receptors. Prostate. 2014; 74:1400–1410. [PubMed: 25132524]

Liu S, Dontu G, Mantle ID, Patel S, Ahn NS, Jackson KW, Suri P, Wicha MS. Hedgehog signaling and Bmi-1 regulate self-renewal of normal and malignant human mammary stem cells. Cancer Res. 2006; 66:6063–6071. [PubMed: 16778178]

Lobo NA, Shimono Y, Qian D, Clarke MF. The biology of cancer stem cells. Annu Rev Cell Dev Biol. 2007; 23:675–699. [PubMed: 17645413]

Low JA, de Sauvage FJ. Clinical experience with Hedgehog pathway inhibitors. J Clin Oncol. 2010; 28:5321–5326. [PubMed: 21041712]

Maclean K, Smith J, St Heaps L, Chia N, Williams R, Peters GB, Onikul E, McCrossin T, Lehmann OJ, Ades LC. Axenfeld-Rieger malformation and distinctive facial features: Clues to a recognizable 6p25 microdeletion syndrome. Am J Med Genet A. 2005; 132:381–385. [PubMed: 15654696]

Magee JA, Piskounova E, Morrison SJ. Cancer stem cells: impact, heterogeneity, and uncertainty. Cancer Cell. 2012; 21:283–296. [PubMed: 22439924]

Mani SA, Guo W, Liao MJ, Eaton EN, Ayyanan A, Zhou AY, Brooks M, Reinhard F, Zhang CC, Shipitsin M, et al. The epithelial-mesenchymal transition generates cells with properties of stem cells. Cell. 2008; 133:704–715. [PubMed: 18485877]

O'Toole SA, Machalek DA, Shearer RF, Millar EK, Nair R, Schofield P, McLeod D, Cooper CL, McNeil CM, McFarland A, et al. Hedgehog overexpression is associated with stromal interactions and predicts for poor outcome in breast cancer. Cancer Res. 2011; 71:4002–4014. [PubMed: 21632555]

Omatsu Y, Seike M, Sugiyama T, Kume T, Nagasawa T. Foxc1 is a critical regulator of haematopoietic stem/progenitor cell niche formation. Nature. 2014; 508:536–540. [PubMed: 24590069]

Ponti D, Costa A, Zaffaroni N, Pratesi G, Petrangolini G, Coradini D, Pilotti S, Pierotti MA, Daidone MG. Isolation and *in vitro* propagation of tumorigenic breast cancer cells with stem/progenitor cell properties. Cancer Res. 2005; 65:5506–5511. [PubMed: 15994920]

Rakha EA, Reis-Filho JS, Ellis IO. Basal-like breast cancer: a critical review. J Clin Oncol. 2008; 26:2568–2581. [PubMed: 18487574]

Ray PS, Wang J, Qu Y, Sim MS, Shamonki J, Bagaria SP, Ye X, Liu B, Elashoff D, Hoon DS, et al. FOXC1 is a potential prognostic biomarker with functional significance in basal-like breast cancer. Cancer Res. 2010; 70:3870–3876. [PubMed: 20406990]

Ricardo S, Vieira AF, Gerhard R, Leitao D, Pinto R, Cameselle-Teijeiro JF, Milanezi F, Schmitt F, Paredes J. Breast cancer stem cell markers CD44, CD24 and ALDH1: expression distribution within intrinsic molecular subtype. J Clin Pathol. 2011; 64:937–946. [PubMed: 21680574]

Robbins DJ, Fei DL, Riobo NA. The Hedgehog signal transduction network. Sci Signal. 2012; 5:re6. [PubMed: 23074268]

Sasaki H, Hui C, Nakafuku M, Kondoh H. A binding site for Gli proteins is essential for HNF-3beta floor plate enhancer activity in transgenics and can respond to Shh *in vitro*. Development. 1997; 124:1313–1322. [PubMed: 9118802]

Sizemore ST, Keri RA. The Forkhead Box Transcription Factor FOXC1 Promotes Breast Cancer Invasion by Inducing Matrix Metalloprotease 7 (MMP7) Expression. J Biol Chem. 2012; 287:24631–24640. [PubMed: 22645147]

Author Manuscript Author Manuscript Author Manuscript Author Manuscript

Sizemore GM, Sizemore ST, Pal B, Booth CN, Seachrist DD, Abdul-Karim FW, Kume T, Keri RA. FOXC1 Is Enriched in the Mammary Luminal Progenitor Population, but Is Not Necessary for Mouse Mammary Ductal Morphogenesis. Biol Reprod. 2013; 89:1–10.

Taipale J, Chen JK, Cooper MK, Wang B, Mann RK, Milenkovic L, Scott MP, Beachy PA. Effects of oncogenic mutations in Smoothened and Patched can be reversed by cyclopamine. Nature. 2000; 406:1005–1009. [PubMed: 10984056]

Wang J, Ray PS, Sim MS, Zhou XZ, Lu KP, Lee AV, Lin X, Bagaria SP, Giuliano AE, Cui X. FOXC1 regulates the functions of human basal-like breast cancer cells by activating NF-kappaB signaling. Oncogene. 2012; 31:4798–4802. [PubMed: 22249250]

Wang Y, Ding Q, Yen CJ, Xia W, Izzo JG, Lang JY, Li CW, Hsu JL, Miller SA, Wang X, et al. The crosstalk of mTOR/S6K1 and Hedgehog pathways. Cancer cell. 2012a; 21:374–387. [PubMed: 22439934]

Wei LX, Zhou RS, Xu HF, Wang JY, Yuan MH. High expression of FOXC1 is associated with poor clinical outcome in non-small cell lung cancer patients. Tumour Biol. 2012; 34:941–946. [PubMed: 23264086]

Wright MH, Calcagno AM, Salcido CD, Carlson MD, Ambudkar SV, Varticovski L. Brca1 breast tumors contain distinct CD44+/CD24− and CD133+ cells with cancer stem cell characteristics. Breast Cancer Res. 2008; 10:R10. [PubMed: 18241344]

Xia L, Huang W, Tian D, Zhu H, Qi X, Chen Z, Zhang Y, Hu H, Fan D, Nie Y, et al. Overexpression of forkhead box C1 promotes tumor metastasis and indicates poor prognosis in hepatocellular carcinoma. Hepatology. 2013; 57:610–624. [PubMed: 22911555]

Yoshida M, Hata K, Takashima R, Ono K, Nakamura E, Takahata Y, Murakami T, Iseki S, Takano-Yamamoto T, Nishimura R, et al. The transcription factor Foxc1 is necessary for Ihh-Gli2-regulated endochondral ossification. Nat Commun. 2015; 6:6653. [PubMed: 25808752]

Yu M, Bardia A, Wittner BS, Stott SL, Smas ME, Ting DT, Isakoff SJ, Ciciliano JC, Wells MN, Shah AM, et al. Circulating breast tumor cells exhibit dynamic changes in epithelial and mesenchymal composition. Science. 2013; 339:580–584. [PubMed: 23372014]

Zvelebil M, Oliemuller E, Gao Q, Wansbury O, Mackay A, Kendrick H, Smalley MJ, Reis-Filho JS, Howard BA. Embryonic mammary signature subsets are activated in Brca1−/− and basal-like breast cancers. Breast Cancer Res. 2013; 15:R25. [PubMed: 23506684]

Author Manuscript Author Manuscript Author Manuscript Author Manuscript

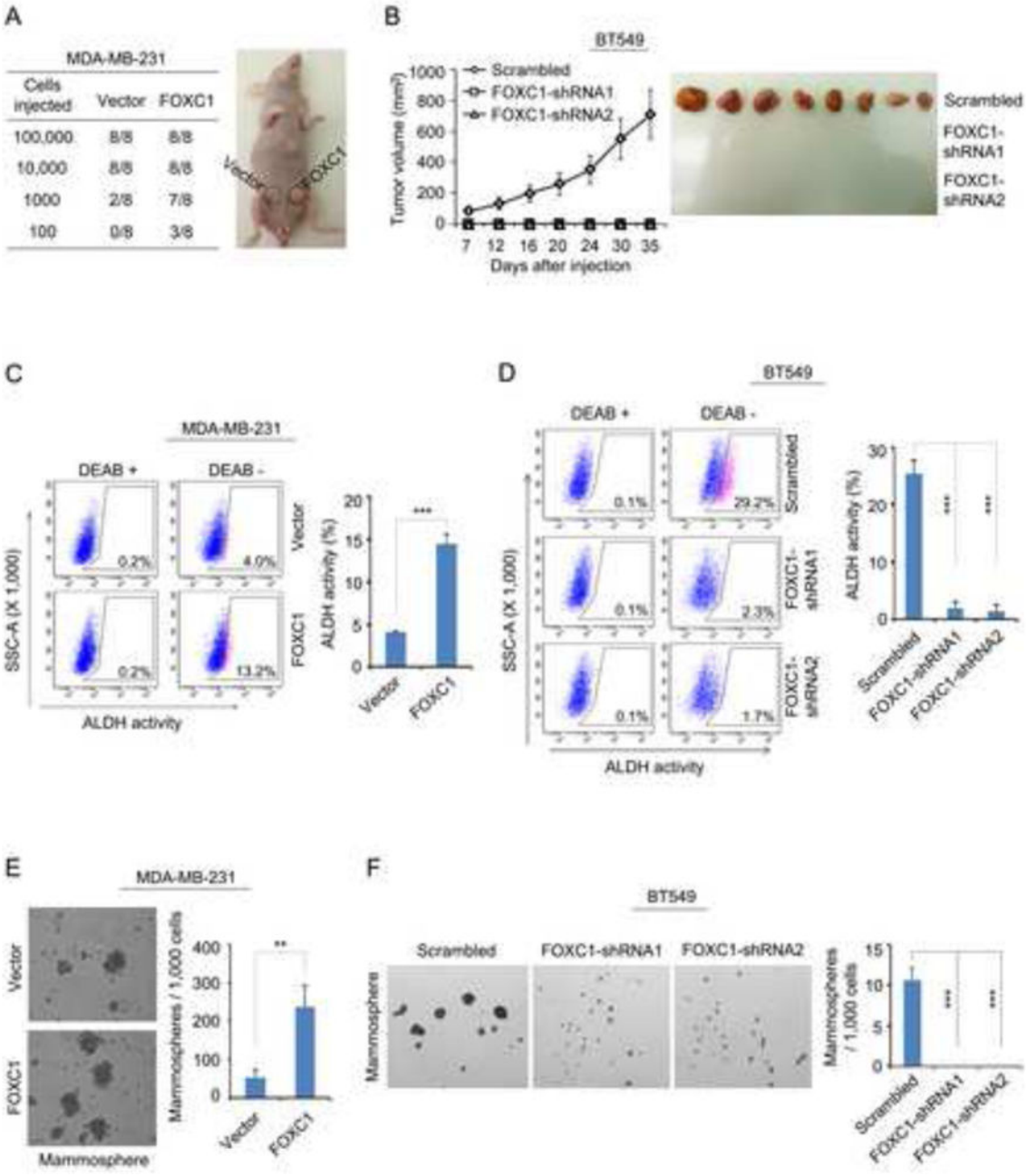

Figure 1. FOXC1 increases CSC properties in BLBC cells *in vivo* and *in vitro*

(A) Tumor incidence rates of different dilutions of control and FOXC1-overexpressing MDA-MB-231 cells injected into the fourth mammary fat pads of BALB/c nude mice.

(B) 3×10^6 control and FOXC1-knockdown BT549 cells were injected into the fourth mammary fat pads of NOD/SCID mice. (n = 8)

(C) Representative flow cytometry analysis of $ALDH^+$ cells in control and FOXC1-overexpressing MDA-MB-231 cells. The bar graph indicates mean ± SD. ***, $p<0.001$.

(D) Representative flow cytometry analysis of $ALDH^+$ cells in control and FOXC1-knockdown BT549 cells. The bar graph indicates mean ± SD. ***, $p<0.001$.

Author Manuscript Author Manuscript Author Manuscript Author Manuscript

(E) Mammosphere growth in control and FOXC1-overexpressing MDA-MB-231 cells. The bar graph indicates mean ± SD. **, $p<0.01$.
(F) Mammosphere growth in control and FOXC1-knockdown BT549 cells. The bar graph indicates mean ± SD. ***, $p<0.001$.
See also Figure S1.

Author Manuscript Author Manuscript Author Manuscript Author Manuscript

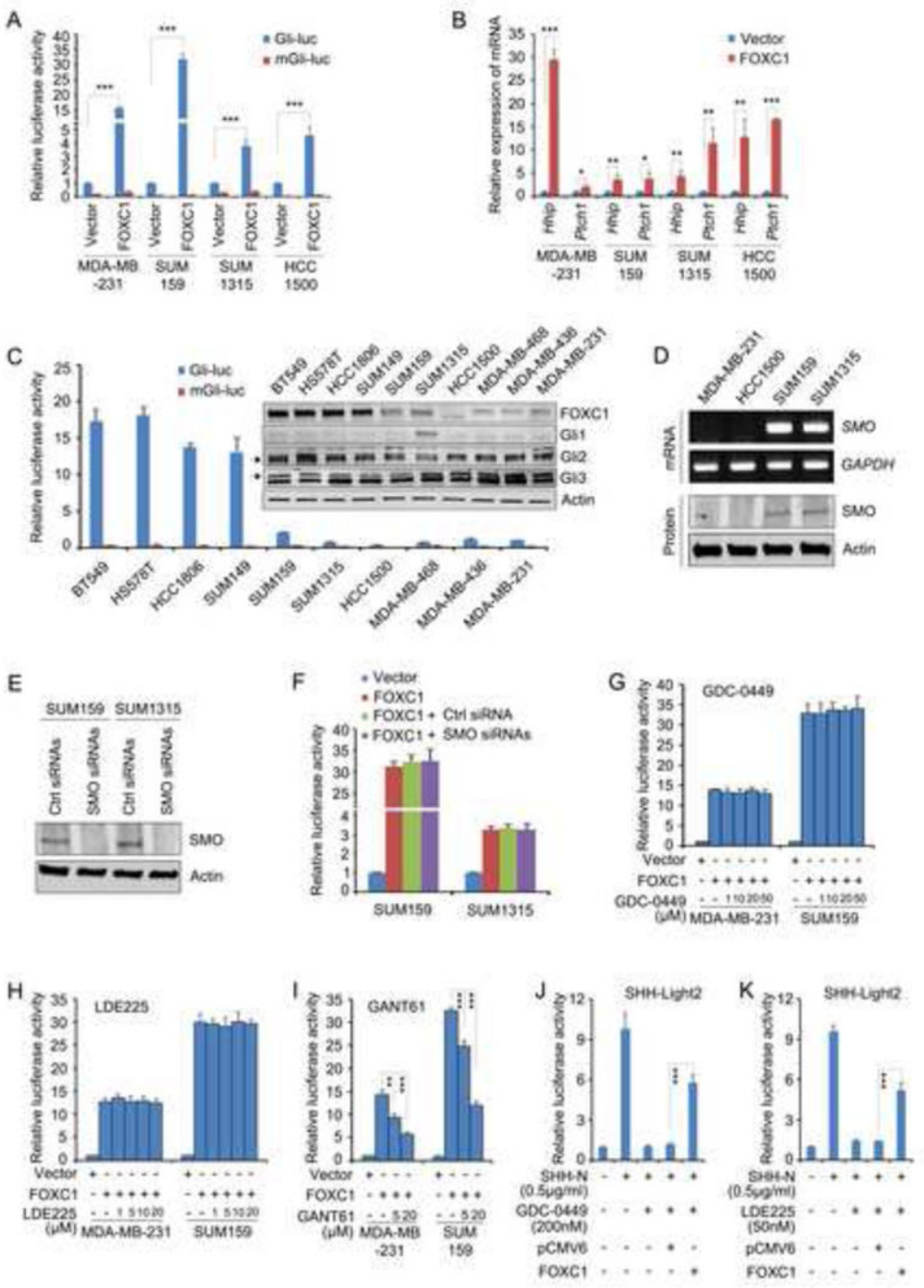

Figure 2. FOXC1 activates SMO-independent Hh signaling in BLBC cells

(A) Cells were transfected with vector or FOXC1 plasmids and wild-type or mutant 8×3′Gli-BS-luciferase plasmids. Luciferase assay was performed. The bar graph indicates mean ± SD. ***, p<0.001.

(B) Real-time PCR analysis of gene expression levels in control or FOXC1-overexpressing BLBC cells. The bar graph indicates mean ± SD. *, p<0.05, **, p<0.01, ***, p<0.001.

(C) Endogenous FOXC1, Gli1, Gli2, and Gli3 protein levels in breast cancer cell lines were measured by western blotting. The same cells were transfected with wild-type or mutant

Author Manuscript Author Manuscript Author Manuscript Author Manuscript

8×3′Gli-BS-luciferase plasmids. Data (mean ± SD) represents relative luciferase activity compared to that in MDA-MB-231 cells.

(D) SMO mRNA and protein levels were measured by RT-PCR and western blotting, respectively.

(E and F) Cells were first transfected with wild-type 8×3′Gli-BS-luciferase and vector or FOXC1 plasmids for 24 h and then were transfected with control or SMO siRNAs for an additional 48 h. SMO knockdown was confirmed by western blotting (E). Luciferase assay was performed (F). The bar graph indicates mean ± SD.

(G–I) Cells were transfected with wild-type 8×3′Gli-BS-luciferase and vector or FOXC1 plasmids. Cells were then treated with GDC-0449 (G), LDE225 (H) and GANT61 (I) at different concentrations for 24 h. Luciferase assay was performed. The bar graph indicates mean ± SD. **, $p<0.01$, ***, $p<0.001$.

(J and K) SHH-Light2 cells were transfected with vector or FOXC1 plasmids. Cells were then treated with SHH-N and GDC-0449 (J) or LDE225 (K). Luciferase assay was performed. The bar graph indicates mean ± SD. ***, $p<0.001$.

See also Figure S2.

Author Manuscript Author Manuscript Author Manuscript Author Manuscript

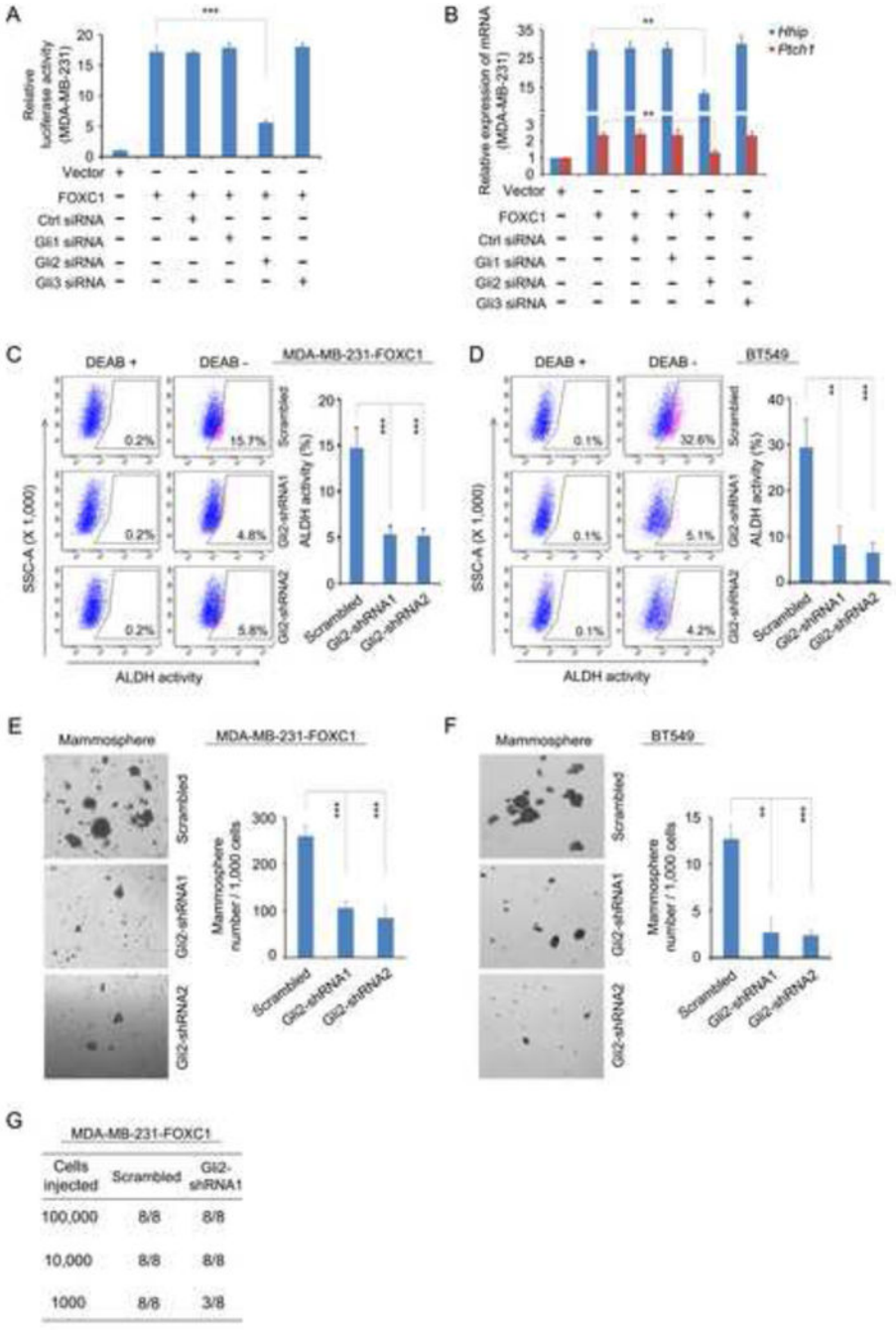

Cells injected	Scrambled	Gli2-shRNA1
100,000	8/8	8/8
10,000	8/8	8/8
1000	8/8	3/8

Figure 3. FOXC1-induced activation of Hh signaling and increase of CSC properties in BLBC cells is mediated by Gli2

(A and B) MDA-MB-231 cells were first transfected with wild-type 8×3′Gli-BS-luciferase and vector or FOXC1 plasmids for 24 h and then transfected with control or Gli1, Gli2, or Gli3 siRNAs for an additional 48 h. Luciferase assay (A) and Real-time PCR (B) were performed. The bar graph indicates mean ± SD (n=3). **, $p<0.01$.

(C) Representative flow cytometry analysis of $ALDH^+$ cells in control or Gli2-knockdown FOXC1-overexpressing MDA-MB-231 cells. The bar graph indicates mean ± SD. ***, $p<0.001$.

Author Manuscript Author Manuscript Author Manuscript Author Manuscript

(D) Representative flow cytometry analysis of $ALDH^+$ cells in control and Gli2-knockdown BT549 cells. The bar graph indicates mean ± SD. **, $p<0.01$, ***, $p<0.001$.
(E) Mammosphere growth in control or Gli2-knockdown FOXC1-overexpressing MDA-MB-231 cells. The bar graph indicates mean ± SD. ***, $p<0.001$.
(F) Mammosphere growth in control and Gli2-knockdown BT549 cells. The bar graph indicates mean ± SD. **, $p<0.01$; ***, $p<0.001$.
(G) Tumor incidence rates of different dilutions of control or Gli2-knockdown FOXC1-overexpressing MDA-MB-231 cells injected into the fourth mammary fat pads of BALB/c nude mice.
See also Figure S3.

Author Manuscript Author Manuscript Author Manuscript Author Manuscript

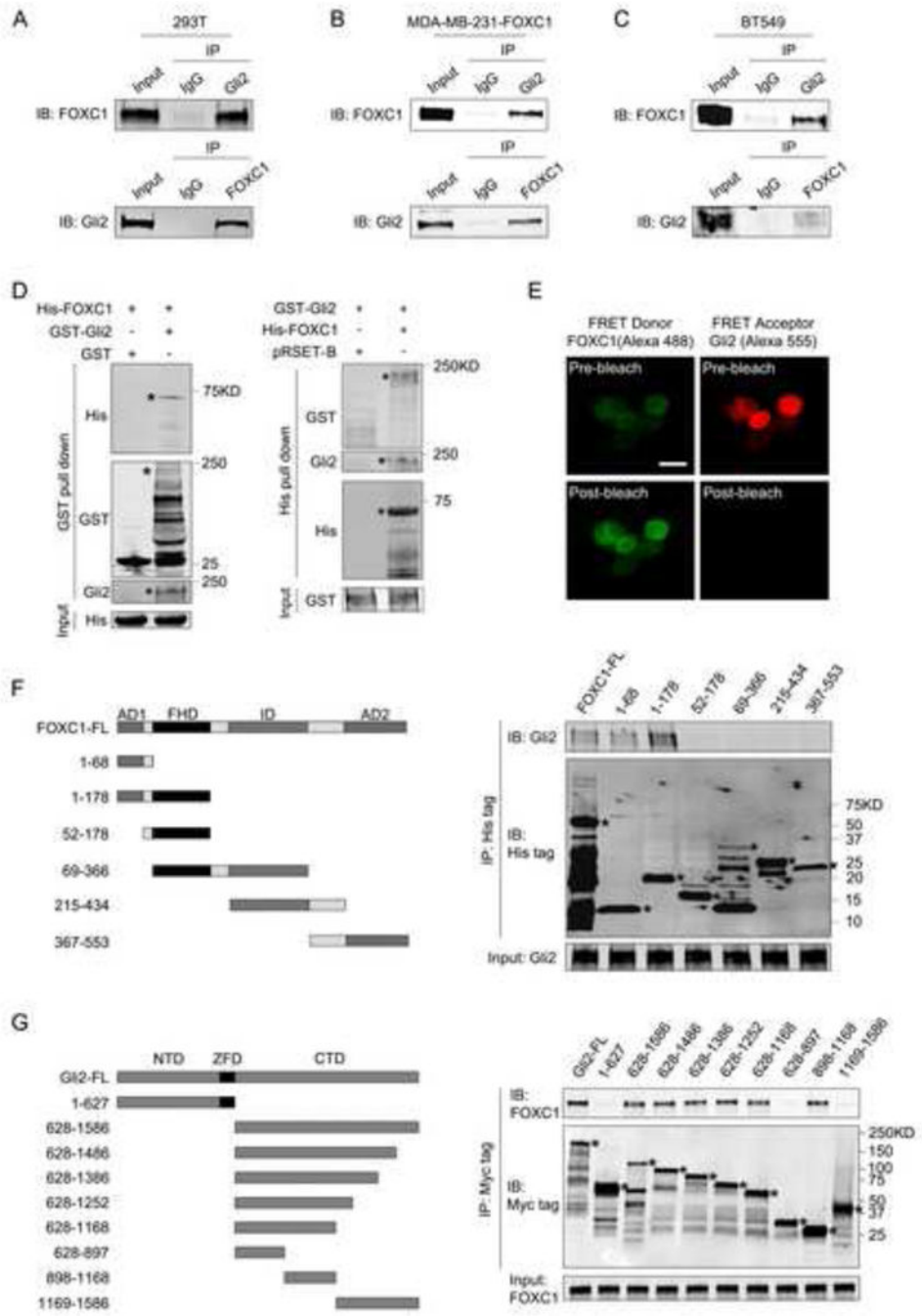

Figure 4. FOXC1 interacts directly with Gli2 in BLBC cells

(A–C) Co-IP analysis of the interaction between FOXC1 and Gli2. Assays were performed in HEK293T cells transfected with both FOXC1 and Gli2 plasmids (A), FOXC1-overexpressing MDA-MB-231 cells (B), and BT549 cells (C).

(D) GST- (left) and His- (right) pull-down assays for the interaction between His-FOXC1 and GST-Gli2. His-FOXC1 and GST-Gli2 were expressed in E. coli BL21 (DE3) and purified.

Author Manuscript Author Manuscript Author Manuscript Author Manuscript

(E) FRET analysis for the direct interaction between FOXC1 and Gli2. HEK293T cells were transfected with FOXC1 and Gli2, followed by immunofluorescence. Scale bar = 25μm.
(F) Illustration of full-length and truncated FOXC1 (left). GST-Gli2 and His-tag full-length or truncated FOXC1 were expressed in E. coli BL21 (DE3). Purified proteins were mixed and subjected to co-IP analysis (right).
(G) Illustration of full-length and truncated Gli2 (left). FOXC1 and Myc-tagged full-length or truncated Gli2 were transfected into HEK293T cells. Proteins were harvested and subjected to co-IP analysis (right).
See also Figure S4–5.

Author Manuscript Author Manuscript Author Manuscript Author Manuscript

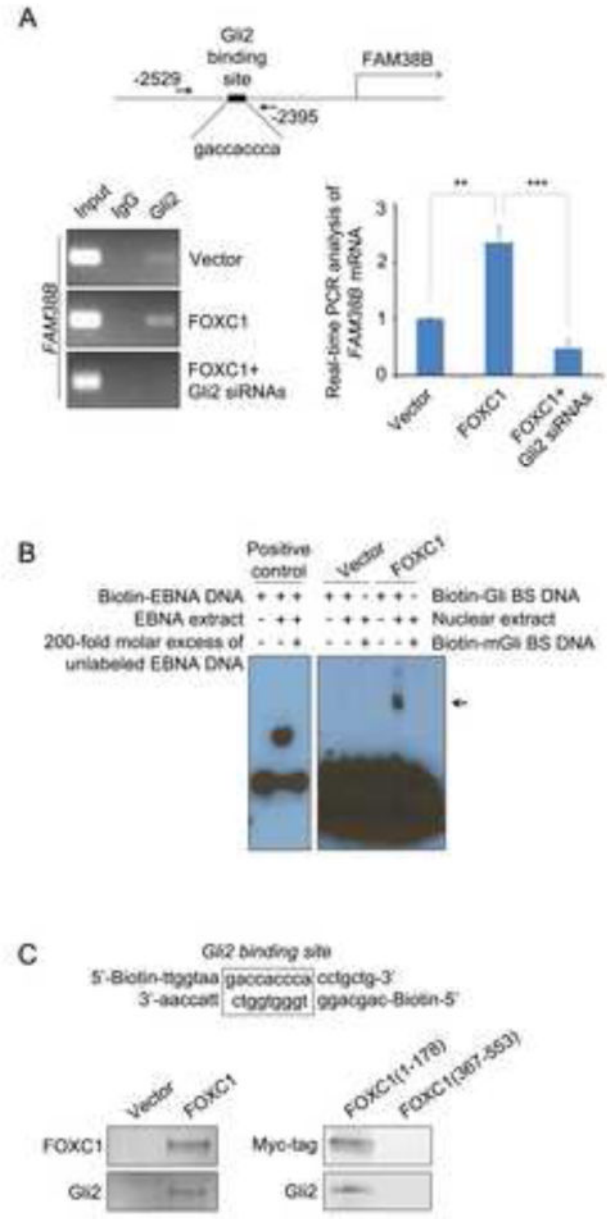

Figure 5. FOXC1 promotes Gli2 DNA-binding capacity

(A) ChIP assay for the binding of Gli2 to the *FAM38B* gene promoter in control, FOXC1-overexpressing, and Gli2-knockdown FOXC1-overexpressing MDA-MB-231 cells. DNA protein complexes immunoprecipitated by Gli2 antibody and IgG were analyzed by RT-PCR and Real-time PCR. The bar graph indicates mean ± SD (n = 3). **, $p<0.01$; ***, $p<0.001$.

(B) EMSA assay for the binding of Gli2 to the *FAM38B* gene promoter in control and FOXC1-overexpressing MDA-MB-231 cells. The Biotin-labeled Gli-binding DNA or mutant Gli-binding DNA was used. Epstein-Barr virus nuclear antigen (EBNA) binding sequence was used as a positive control.

(C) Biotinylated oligonucleotide precipitation assay for the binding of Gli2 to the *FAM38B* gene promoter in control and FOXC1-overexpressing MDA-MB-231 cells (left), and in

MDA-MB-231 cells transfected with FOXC1 truncates (right). The Biotin-labeled Gli-binding DNA was used.

Author Manuscript Author Manuscript Author Manuscript Author Manuscript

Author Manuscript Author Manuscript Author Manuscript Author Manuscript

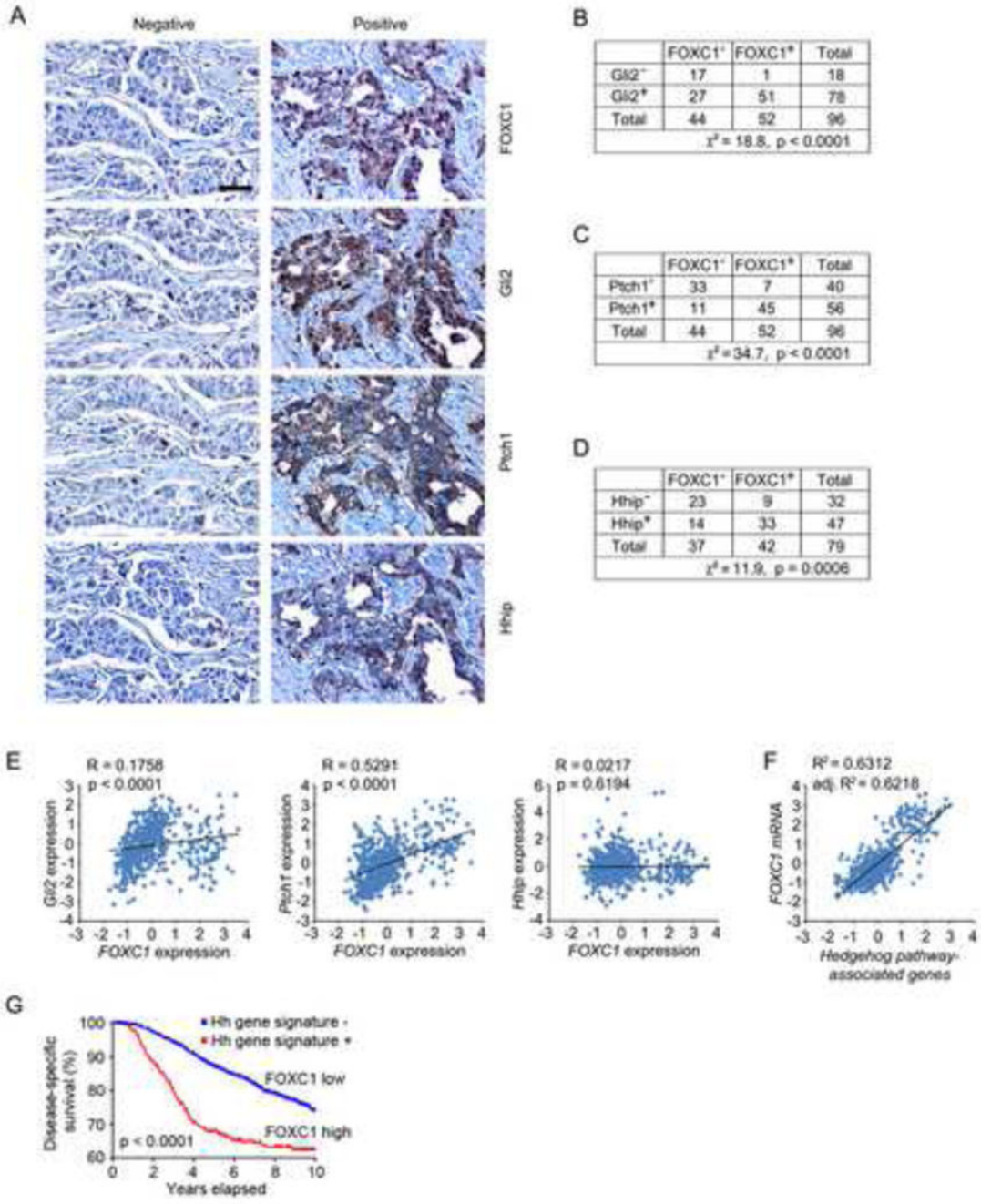

	FOXC1⁻	FOXC1⁺	Total
Gli2⁻	17	1	18
Gli2⁺	27	51	78
Total	44	52	96
	$\chi^2 = 18.8$, $p < 0.0001$		

	FOXC1⁻	FOXC1⁺	Total
Ptch1⁻	33	7	40
Ptch1⁺	11	45	56
Total	44	52	96
	$\chi^2 = 34.7$, $p < 0.0001$		

	FOXC1⁻	FOXC1⁺	Total
Hhip⁻	23	9	32
Hhip⁺	14	33	47
Total	37	42	79
	$\chi^2 = 11.9$, $p = 0.0006$		

Figure 6. FOXC1 correlates with Hh pathway activation in clinical samples

(A) Representative IHC results in TNBC tissue microarray samples. Scale bar = 50μm.

(B–D) Correlation analysis of FOXC1 and Gli2 (B), FOXC1 and Ptch1 (C), and FOXC1 and Hhip (D) based on the IHC staining results. Linear regression analysis was performed.

(E) Correlation analysis between FOXC1 and Gli2, Ptch1, Hhip in TCGA samples (n = 526). Linear regression analysis was performed.

Author Manuscript Author Manuscript Author Manuscript Author Manuscript

(F) Correlation analysis between FOXC1 and 13 Hh pathway-associated genes (see Statistics section in Methods) in TCGA samples (n = 526). Multiple regression analysis was performed.

(G) Kaplan Meier curves of % disease-specific survival of two groups of patients from the Curtis dataset that were either positively (n=378) or negatively (n=1608) enriched for the 13 Hh pathway-associated genes. Log-rank test was performed to calculate p value.

See also Figure S6.

Author Manuscript Author Manuscript Author Manuscript Author Manuscript

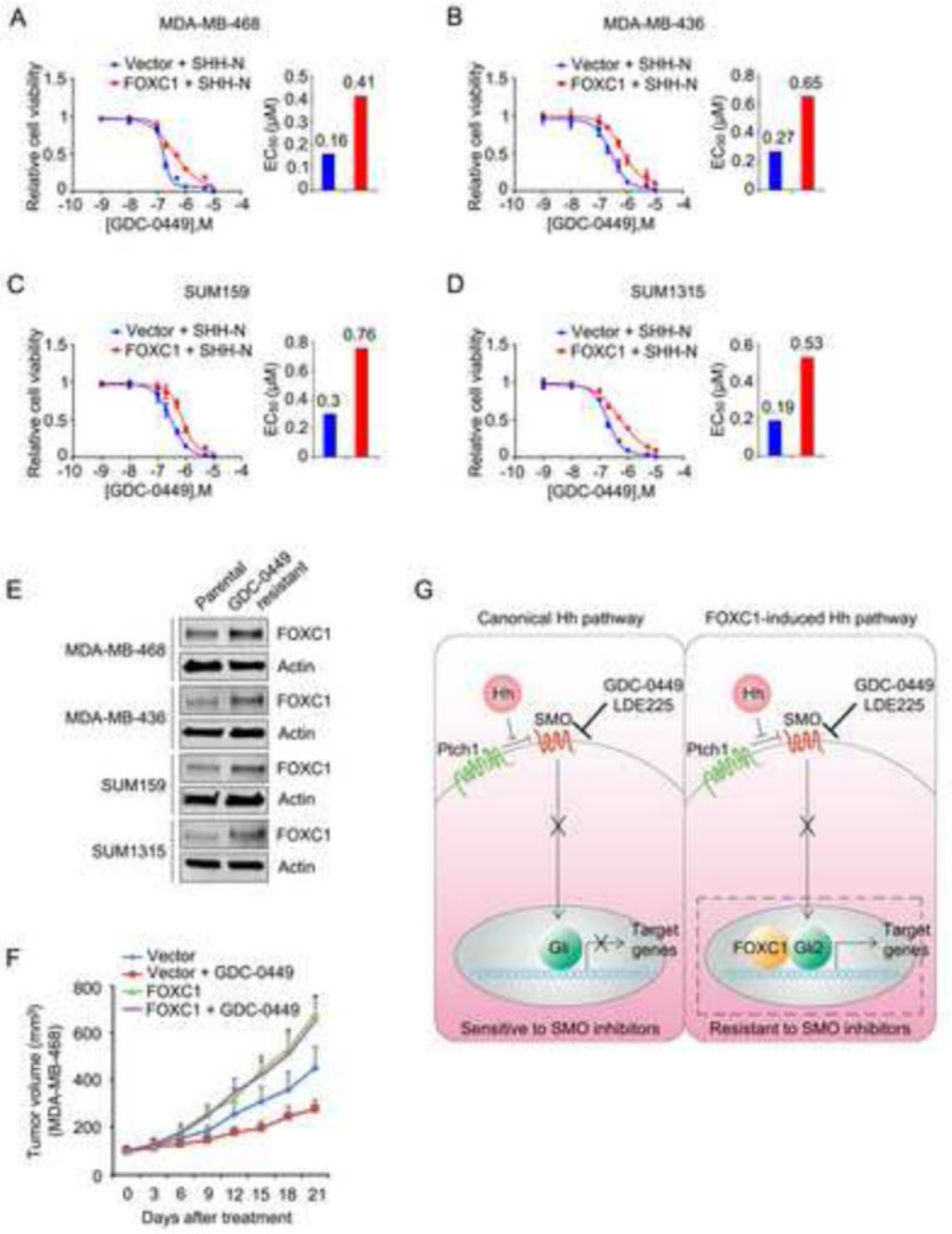

Figure 7. FOXC1 induces resistance to anti-Hh drug

(A–D) Relative cell viability and EC_{50} of GDC-0449 in control or FOXC1-overexpressing MDA-MB-468 cells treated with the recombinant N-terminal fragment of the Sonic hedgehog protein (SHH-N) (A), MDA-MB-436 cells (B), SUM159 cells (C), and SUM1315 cells (D). Data represents mean ± SD of three separate experiments.

(E) Expression levels of FOXC1 protein in different parental and *in vitro* derived GDC-0449-resistant BLBC cells.

Author Manuscript Author Manuscript Author Manuscript Author Manuscript

(F) 5×10^6 control or FOXC1-overexpressing MDA-MB-468 cells were injected into the fourth mammary glands of BALB/c nude mice (n = 10 per group). When tumors reached $100mm^3$, mice were treated with GDC-0449 daily at a dose of 250 mg/kg by oral gavage. Data represents mean ± SD.

(G) Schematic diagrams for the canonical and FOXC1-induced SMO-independent Hh signaling pathways.

See also Figure S7.